Lysine-independent ubiquitination and degradation of REV-ERBα involves a bi-functional degradation control sequence at its N-terminus.

Ting-Chung Suen and Jason P. DeBruyne

Department of Pharmacology and Toxicology, Neuroscience Institute, Morehouse School of Medicine, 720 Westview Drive SW, Atlanta, GA 30310, USA

Running title: A degradation control region on REV-ERBα protein

Keywords: REV-ERBα, Lysine-independent, ubiquitination, degradation, proteasome

Abstract

REV-ERBα and REV-ERBβ are important components of the mammalian circadian clock and play a crucial role in linking the circadian system to overt daily rhythms in physiology and behavior. Expression of these parologs is driven by the circadian clockwork, and in most tissues, the abundance of REV-ERBα proteins robustly cycles such that they are detected only within a tight interval of 4-6 hours each day, suggesting control of both their synthesis and degradation are tightly controlled. Several ubiquitin ligases have been shown to mediate REV-ERBα degradation, but how they interact with REV-ERBα and which lysine residues they ubiquitinate to drive its degradation are unknown. In this study, we attempted to identify both ubiquitin-ligase-binding and ubiquitination sites within REV-ERBα required for its degradation. Surprisingly, a REV-ERBα mutants with all its 20 lysines changed to arginine (K20R) can be efficiently ubiquitinated and degraded in the absence or presence of two E3 ligases, SIAH2 and SPSB4, suggesting possible N-terminal ubiquitination. To explore this, we examined if small deletions at the N-terminus of REV-ERBα will alter its degradation. Interestingly, deletion of amino acid (AA) residues 2 to 9 (delAA2-9) clearly resulted in a less stable REV-ERBα. We found that it was the length (i.e. 8 AA), and not the specific sequence, that confers stability in this region. Simultaneously, we also mapped the interaction site of the E3 ligase SPAB4 to this same regions, specifically requiring AA4-9 of REV-ERBα. Thus, the first 9 AA of REV-ERBα has two opposing roles in regulating REV-ERBα turnover. Further, deleting eight additional AAs (delAA2-17) from REV-ERBα almost prevents its degradation. Combined, these results suggest that complex interactions within the first 25AAs potentially act as a REV-ERBα 'switch' that allows a protected/stabilized conformation to accumulate at one time of day, but then rapidly shifts to a destabilized form, to enhance its removal at the end of the daily cycle.

Introduction

Proper functioning of the circadian clock depends on timely expression of multiple transcription factors that comprise a set of interlocking transcriptional-translational negative feedback loops (1-3). REV-ERBα and REV-ERBβ are transcriptional repressors that are important components of the mammalian circadian clock (4-7). Expression of *Rev-Erbα* at the RNA level is robustly rhythmic, and REV-ERBα protein is only detectable within a 4-hour interval during the day (4). The tight interval of REV-ERBα protein existence in the cells highlights the significance of its rapid elimination from the cells at the appropriate time. However, the mechanisms of how such fast degradation is accomplished at the appropriate time is unknown.

Most proteins in the cells are eliminated by the ubiquitin-proteasome (UPS) system, where chains of ubiquitin molecules are covalently attached to one or more lysine residues on proteins targeted for degradation. This important first step of protein degradation is achieved through the concerted actions of a cascade of enzymes, E1 ubiquitin activating enzymes, E2 ubiquitin conjugating enzymes, and E3 ubiquitin ligases (8-10). Ubiquitin ligases provide specificity on which proteins are to be targeted and degraded by the proteasome (11). Our laboratory developed a functional screen (12) that could identify which ubiquitin ligase(s) is responsible for degrading a specific protein of interest. SIAH2, SPSB1, and SPSB4 were identified in this screening strategy to strongly accelerate the degradation of REV-ERBα (12). Depletion of SIAH2, SPSB1, and SPSB4 resulted in the alteration of REV-ERBα level and suppression of its downstream target genes, as well as the overall circadian oscillator function (12, 13), indicating timely degradation of REV-ERB is important for proper clock function. Interestingly, SIAH2 knockout mice revealed itself as a female-specific regulator of circadian rhythms and metabolism, although the role of REV-ERBα was unclear (14). Other ubiquitin ligases, Arf-bp1 and Pam (15), FBXW7 (16), have also been reported to drive degradation of REV-ERBα. Removal of each of these E3 ligases have distinct effects on REV-ERBα stability and overall clock function, suggesting that each serves a specific, non-overlapping role in REV-ERBα degradation. To understand how these E3 ligases

may cooperate, in this study, we focused on identifying the basic regulatory mechanisms on the REV-ERBα protein itself. In other words, what changes are needed to happen to the REV-ERBα protein before it undergoes the process of degradation?

We initially tried to determine if certain lysine residues on the mouse REV-ERBα protein are targets of ubiquitin attachment, and subsequent degradation through the 26S proteasome (17-19). Surprisingly, even when all twenty of its lysine's were mutated to arginines (K20R), there was no substantial difference in the ubiquitination of K20R when compared to the wildtype (WT) protein. Although K20R exhibited a slow-down in degradation, it was still degraded rather efficiently. As ε-amino group on a lysine residue is commonly reported as the predominant site of attack by ubiquitin ligases (9,17), the most likely site of ubiquitin conjugation on K20R would be the only free α-amino group left at the methionine located at the very N-terminus of the protein. Small deletions were therefore introduced at the N-terminus to test if they would affect degradation. Interestingly, deletion of amino acid (AA) residues 2-9 (delAA2-9, the N-terminal methionine being the first AA) resulted in an unstable REV-ERBα, while extending the deletion for eight more amino acids (delAA2-17) resulted in a much more stable protein.

This degradation control region became even more complicated as we found that AA4-9 is the binding site for SPSB4, an E3 ubiquitin ligase that we showed previously to degrade REV-ERBα, but not REV-ERBβ (12). It appears counterintuitive when the removal of an ubiquitin ligase binding site (AA2-9) would make the protein less stable. Nevertheless, the combined data may reveal a more complex regulatory role of AA2-9 in controlling REV-ERBα degradation. First, it serves as the binding site for SPSB4 such that REV-ERBα can be ubiquitinated and brought to the proteasome. Once REV-ERBα is bound to the proteasome, AA2-9 may serve as a final gatekeeper to impede the protein from the actual degradation process. This novel dual-functioning domain potentially could control the timing of when to initiate acceleration of degradation of REV-ERBα when the protein is no longer needed. The identification of this novel degradation-control region is very exciting as it provides a first handle to investigate the mechanism of how REV-ERBα is stable during time of the day when it is needed to perform its functions as a regulator of the circadian clock.

Materials and Methods

Cell lines and transfection.

The human embryonic kidney cell line HEK293 was maintained in Dulbecco's modified Eagle's medium (DMEM) with 10% fetal bovine serum, in a 37^0C humidified incubator with 5% CO2. Transfection was carried out with Fugene HD (Promega, Madison, WI) or Lipofectamine 2000 (Fisher Scientific, Waltham, MA) according to manufacturer's instructions.

Plasmids and mutants

pCMVSport6Rev-Erbα contains the mouse *rev-erbα* cDNA cloned into the mammalian expression vector pCMVSport6. In vitro mutagenesis was carried out with the Q5 site-directed mutagenesis kit (New England Biolabs, Ipswich, MA). Primers specific for the appropriate mutations were designed with the NEBaseChanger on the NEB website, and were purchased from Thermo Fisher Scientific (Waltham, MA). Briefly, 10ng of plasmid was mixed with 1μM of a specific primer pair, along with the enzyme mix provided. PCR was carried out as described in the mutagenesis protocol with melting temperature selected for the specific primer pair. PCR products were then checked by agarose gel electrophoresis. Products with correct size were treated with a mixture of enzymes including kinase, ligase, and Dpnl (KLD mix) for 10 minutes, such that the original plasmid would be digested to reduce background during transformation. 1μl of the KLD-treated newly synthesized plasmid was used to transform the DH5α strain of E. coli provided. Colonies were picked and grown overnight in Luria Broth medium with appropriate antibiotics, plasmids were isolated with Qiagen (Germantown, MD) Plasmid Mini Kit, and DNA were sent for sequencing with appropriate primer to confirm if the specific mutation was successfully introduced.

Primers
Oligonucleotides or primers were purchased from Thermo Fisher Scientific (Waltham, MA). Information for all primers will be available upon request.

Sequencing
Sequencing was performed either by the Core Facility of Morehouse School of Medicine (MSM) or Eurofins Genomics (Louisville, KY), with primer chosen specifically to verify if the intended mutations were successfully obtained.

Antibodies
Antibodies were obtained from Cell Signaling Technology (Danvers, MA). These include anti-Rev-Erbα (Cat No. 13418S), anti-GAPDH (Cat. No. 5174S), anti-β-Actin (Cat. No. 4970S), anti-HA-Tag (rabbit, Cat. No. 3724S, and mouse, Cat. No. 2367S), anti-MYC-tag (rabbit, Cat. No. 2278S, and mouse, Cat. No. 2276S), HRP-conjugated secondary antibodies include Goat anti-mouse IgG (Cat. No. 91196) and anti-rabbit IgG (Cat. No. 7074). Fluorescence conjugated secondary antibodies were purchased from Fisher Scientific (Waltham, MA), these include Invitrogen goat-anti-rabbit (Cat. No. PIA32735) or goat-anti-mouse (Cat. No. PIA32730) Alexa Fluor Plus 800, goat-anti-rabbit (Cat. No. PIA32734) or goat-anti-mouse (Cat No. PIA32729) Fluor Plus 680. Protein-A agarose beads (Cat No. 9863S) were also products of Cell Signaling Technology.

Protein degradation assays
Typically, HEK293 cells were washed with Phosphate Buffered Saline (PBS, Cytiva HyClone Cat. No. BSS-PBS-1X6), trypsinized (Corning 0.25% Trypsin), collected with DMEM, and centrifuged (1500 rpm, 5 minute). Cells were resuspended in fresh medium, counted, and seeded into a 24-well plate (Corning Falcon 353047) at a density of 10^5 cells per well. 100 ng of plasmids that express the cDNA of either the wildtype (WT) or mutant REV-ERBα were transfected into multiple wells with Fugene HD (Promega, Madison, WI) or Invitrogen Lipofectamine 2000 (Fisher Scientific). For experiments on ubiquitin ligase-induced degradation, 50 ng of empty vector pCMVSport6, SIAH2-, or SPSB4-expressing plasmid, was added to the 100ng of REV-ERBα expressing plasmid. 36-48 hours after transfection, cells were treated with cycloheximide (Cat. No. 2112S, Cell Signaling, Danvers, MA) at 10 μg/ml final concentration for various times as indicated in individual experiments. The proteasome inhibitor MG132 (Cat. No. 2194S, Cell Signaling, Danvers, MA) was also added to one of the well at a final concentration of 5μM, usually treated along with the longest time point of cycloheximide. Cells were washed with PBS, followed by lysis with 100μl of RIPA buffer (diluted from a 2X solution, Cat. No. BP115X, Boston Bioproducts Inc., Ashland, MA), supplemented with a protease inhibitor cocktail (Cat. No. 5871S, Cell Signaling, Danvers, MA), at 4^0C on a rocking platform. Cell lysates were collected after one to two hour and transferred from the individual wells into microcentrifuge tubes. Cell debris were cleared by centrifugation at 13,000 rpm in a microcentrifuge at 4^0C for 15-30 minutes. Supernatants were then transferred to new tubes and either stored at -80^0C, or were ready for Western analysis.

Western blots
Aliquots of cell lysates were mixed with appropriate amount of a 6X SDS-Sample buffer, reducing (Cat. No. BP-11R, Boston Bioproducts Inc., Ashland, MA), heated to 95^0C for 5 minutes, before being loaded onto a Bio-Rad Criterion TGX or mini-PROTEAN TGX gel, and run with the Criterion Vertical Electrophoresis Cell system (Bio-Rad, Hercules, CA). Proteins were then transferred to Cytiva Amersham Hybond PVDF membranes (formerly GE Healthcare Life Sciences, now Global Life Sciences Solution USA LLC, Marlborough, MA) using the Bio-Rad Trans-Blot Turbo transfer system. Membranes were washed for 5 minutes at room temperature on an orbital shaker with 1X Tris-buffered saline (TBS), diluted from a 20X TBS stock solution (Cat. No. BM300X, Boston Bioproducts Inc., Ashland, MA). Blocking was followed by placing the membrane in 1X TBS with 5% non-fat dry milk or bovine serum

albumin (BSA) (Boston Bioproducts Inc., Ashland, MA, on a rocking platform, at 4^0C. After an hour, an appropriate antibody in TBST (TBS with 0.1% Tween-20) with 5% of either non-fat dry milk or BSA was then incubated with the membrane on a rocking platform at 4^0C. After overnight incubation, membranes were washed with 1X TBST for 10 minutes at room temperature on an orbital shaker. After 3 washes, appropriate secondary antibody in TBST was added and left shaking for 1 hour at room temperature on the rotating platform. Three washes with TBST were then carried out as before. Membranes were exposed to chemiluminescence when HRP-conjugated antibody was used, while imaging was obtained with LI-COR Odyssey Fc Imaging system (LI-COR, Lincoln, NB) when fluorescein-conjugated antibodies were used.

Immunoprecipitation

Typically, 500 ng of the plasmid vector pCMVSport6, pCMVSport6REV-ERBα-WT or mutants were transfected into different wells of a 6-well tissue culture plate (Corning Falcon 353046), with either 250ng of pCMVSport6 or pCMVSport6-HA-Ub, a plasmid that expresses a HA-tagged ubiquitin. 36-48 hours after transfection, cells were changed into medium containing 5 μM MG132 (Cat. No. 2194S, Cell Signaling, Danvers, MA). 2-3 hours later, cells were washed with 2-ml PBS followed by the addition of 300μl trypsin. Detached cells were collected into 15 ml conical tubes with 4ml of medium. Cells were centrifuged at room temperature for 5 minutes at 1,500rpm. The supernatants were removed, and the cell pellets were resuspended with 1.5ml PBS and transferred to microcentrifuge tubes. Cells were centrifuged at 1,500rpm for 5 minutes in 4^0C, PBS was aspirated off and the pellets were resuspended with 150μl of RIPA buffer with protease inhibitors. The tubes were then left on a rocking platform at 4^0C for 1-2 hours. Cell lysates were then cleared by spinning at 13,000rpm for 30 minutes at 4^0C, after which a 10 μl aliquot was transferred to a tube with 2 μl of Laemmli 6X SDS-Sample buffer and stored as input lysate in -80^0C. The remaining cell lysates were added to Eppendorf tubes containing 650 μl of PBST (phosphate buffered saline with 0.1% Tween-20) with protease inhibitor cocktail, along with 10 μl of pre-washed Protein-A Agarose beads (Cat. No. 9863S, Cell Signaling, Danvers, MA). The tubes were left on a rotating disc at 4^0C overnight for pre-clearing the lysates. The agarose beads were spun down at 4,000rpm for 3 minutes in a microcentrifuge at 4^0C. Cell lystaes were then transferred to low-protein binding Eppendorf tubes (Cat. No. 13-698-794, Fisher Scientific) containing 3 μl of anti-REV-ERBα antibody. Tubes were placed back to the rotating disc at 4^0C for 4-8 hours, after which a fresh 15 μl of Protein-A Agarose beads were added. The tubes were again placed back onto the rotating disc overnight. The immunoprecipitated mix was centrifuged at 4,000 rpm for 3 minutes, supernatant removed, and fresh PBST was added to wash the agarose beads with the tubes back onto the rotating disc. Centrifugation and washing were repeated 3 more times. Supernatant was carefully removed as much as possible after the last wash. 25 μl of 6X SDS-Sample buffer, reducing loading dye, were added to the beads. The immunoprecipitated mix, along with the input lysates aliquoted the day before were heated to 95^0C for 10 minutes, vortexed briefly and spun down in microcentrifuge, before being loaded on a gel for Western.

Results

Lysine-independent degradation of REV-ERBα

Since the first step to mark a protein for degradation is the addition of a chain of ubiquitin molecules to one or more lysine residues on the protein (8-10), our initial approach was to try to identify which lysine residues are important for the degradation of REV-ERBα. A simple schematic illustration of the mouse REV-ERBα protein is shown in Figure 1A, with the DNA-binding and ligand-binding domains shown as shaded and open boxes, respectively. The relative positions of all lysine residues are indicated by “K”s (not drawn to scale). Three ubiquitinated peptides were found and mapped in an ubiquitinome study (20) to lysines at amino acid (AA) positions 456, 577, and 592 (the three underlined “K”s in Figure 1A) on

REV-ERBα. These 3 lysines were therefore mutated to arginines (R), both individually and in combinations. When these mutants were transfected into HEK293 cells, their degradation profiles in a cycloheximide time course were compared to the wildtype (WT) protein, and only minor changes in their rate of degradation were detected (data not shown). We ended up having to mutate all twenty lysines on REV-ERBα to arginines, (the K20R mutant in Figure 1A), expecting to see a big change in protein stability. To our surprise, although altering all lysine residues delay the degradation of REV-ERBα (Figure 1B, compare lanes 9-15 to lanes 1-7). The mutant protein is still efficiently degraded at the end of the time course (Figure 1C). The degradation was clearly mediated by proteasome as the level of REV-ERBα was maintained after 6 hours when the proteasome inhibitor MG132 (lanes 'M') was added to the cells (lanes 8 and 16 compared with lanes 1 and 9, respectively). Thus, although lysine ubiquitination is known to be the major and essential initiation event that leads to protein degradation by the proteasome (17), the above results clearly showed that ubiquitination on lysine residue is not needed for proteasome-mediated degradation of REV-ERBα.

Lysine-independent ubiquitination of REV-ERBα

The slowdown but efficient degradation of K20R prompted us to test if it could still be ubiquitinated when compared to the WT protein under identical conditions. Both WT and K20R were expressed in HEK293 cells (Figure 1D, "Input" lanes 1-4), with ("+" lanes) or without ("-" lanes) co-transfection of a plasmid that expresses a HA-tagged ubiquitin cDNA (HA-Ub). Cells were lysed and followed by immunoprecipitation (IP) with anti-REV-ERBα antibody (lanes 7-18). Western blot using anti-REV-ERBα antibody (lanes 1-12) showed that similar amount of WT and K20R were successfully brought down by IP (lanes 7-10), while endogenous REV-ERBα was undetectable in non-transfected HEK293 cells (lanes 5, 6, 11, 12). When anti-HA antibody was used (lanes 13-18), bands appear as ladders (marked by bracket) were detected only in those lanes where HA-Ub were also co-transfected (lanes 14 and 16). The absence of these ladders in the HEK293 cells (lanes 17 and 18) further confirmed their specificity. These bands all have higher molecular weight than that of REV-ERBα (around 75kD, bands at 50kD are immunoglobulin heavy chain), suggesting that they are REV-ERBα with increasing numbers of ubiquitin molecules attached, as each additional ubiquitin molecule would increase the size of the protein by 8kD. Importantly, the ladder of bands detected in K20R (lane 16) suggested that it is also efficiently ubiquitinated even though it does not even have a single lysine. This result was intriguing as the ε-amino group on lysine is known to be the site where ubiquitin attaches to proteins. Nevertheless, the ability of K20R to be ubiquitinated is consistent with the fact that it can be degraded efficiently (Figures 1B and 1C).

Our laboratory previously identified several ubiquitin ligases, SIAH2, SPSB1, and SPSB4 (12, 13), that were able to accelerate the degradation of REV-ERBα when they were co-expressed. Depletion of these E3 ligases also resulted the suppression of target genes downstream of REV-ERBα, as well as an extended circadian period, (12, 13). It's commonly accepted that E3 ligases function to ubiquitinate proteins on lysine residue(s), we therefore tested if E3-induced degradation of REV-ERBα was affected in the K20R mutant. Consistent with results in Figures 1B and 1C, the K20R mutant is relatively stable in the first 4 hours (Figure 1E, lanes 1-8). When SPSB4 was co-expressed, K20R degradation was clearly accelerated (lanes 9-16). SIAH2's ability to degrade K20R appeared to be much more potent than SPSB4, as only weak signals of K20R were detected (lanes 17-24). These data added more surprises about the role of lysine in protein degradation but it also supports further that ubiquitination and degradation of REV-ERBα is indeed lysine-independent.

N-terminus of REV-ERBα controls its degradation

Since the ε-amino group on a lysine residue is commonly reported for most proteins as the predominant site of attack by ubiquitin ligases (8-10), a likely site of ubiquitin conjugation on the K20R mutant would

be the only free α-amino group on the methionine located at the very N-terminus of the protein. The fact that two ubiquitin ligases were able to strongly induce degradation of K20R (Figure 1E) also supports this possibility. We reasoned that if the N-terminus is important for ubiquitination, perhaps altering the amino acids in its proximity would affect degradation. Since the N-terminal methionine is the translation initiation site that needs to be preserved, we introduced small deletions of 8 to16AAs near the N-terminus, (Figure 2A, the methionine is marked as "M" and is numbered "1" as it is the first amino acid (AA) of the protein. The next 24 AAs are shown as three different colored blocks of 8AAs, with their boundaries being 2-9, 10-17, and 18-25, respectively, as marked. The remainder of the protein is shown as a green ellipse, not drawn to scale. The sequence of the first 30AAs with matching color blocks is shown underneath). As shown in the western blot (Figure 2B), the mutant delAA2-9 (lanes 9-16) clearly degraded faster than the WT (lanes 1-7, and densitometry quantitation shown in Figure 2C) Interestingly, extending the deletion to 16AAs (mutant delAA2-17) resulted in a much more stable protein (lanes 17-23, and Figure 2C). The degradation of delAA2-9 mutant, like the WT protein, appears to be mediated by the proteasome, since the level of protein remained after 10 hours in the presence of MG132 was close to the level found at time 0 (compare lane 8 to lane 1 for WT, lane 16 to lane 9 for delAA2-9). On the contrary, the presence of MG132 was not able to rescue the level of delAA2-17 mutant back to the level found at time 0 (compare lane 24 to lane 17). Instead, the level of delAA2-17 found after 10 hours of MG132 treatment (lane 24) was very similar to the level found after 10 hours of cycloheximide treatment (lane 23). These results suggested that the slow degradation of delAA2-17 (lanes 17-23) being observed was not mediated by proteasome. Overall, the combined results indicated that the N-terminus of REV-ERBa contains a small domain that plays an important role in regulating its degradation.

Characterization of how AA2-9 may prevent fast degradation REV-ERBα

The removal of AA2-9 from the N-terminus of REV-ERBα clearly resulted in an unstable protein (delAA2-9, Figure 2), suggesting that AA2-9 may have a role in slowing down degradatation when the protein is in its native conformation. To examine if there is a sequence requirement for AA2-9 to impede degradation, successive pairs of AA2-3, 4-5, 6-7, or 8-9, respectively, were mutated to double alanines (Figure 3A) and their stability were tested. As shown in Figures 3B and 3C, no discernable difference could be seen with all these substitution mutants when compared to the wild type (lanes 1-6; lane "0" in Figure 3C was the same sample used in lane 1 of Figure 3B to allow better comparison across the two membranes). Results from the above experiments suggested that there is no strict amino acid sequence requirement for AA2-9 to block fast degradation. On the other hand, perhaps when only 6 out of the original 8 amino acids are in place, the protein will be maintained as WT-like. Next, we examined two additional mutants, both maintaining the same composition of the eight amino acids within AA2-9, but they were re-arranged in different orders (Figure 3D, AA1-9 are numbered accordingly in the WT, with their orders rearranged in the mutants). As shown in Figure 3E, reversing the native order of AA2-9 to AA9-2 (RevAA9-2, lanes 7-12) did not change the rate of degradation. The other mutant with the order of AA2-9 scrambled (SCRAM-AA2-9) appeared to be degraded slightly faster (lanes 13-18) than the WT (lanes 1-6), but nothing near the rapid degradation that was clearly observed with delAA2-9 (Figure 2). These data suggest the composition of amino acid residues within AA2-9, but not the exact order, is important for it to block fast degradation. The discovery of the degradation-blocking activity of AA2-9 originated from considering the possibility of N-terminal ubiquitination, we therefore tested if shortening the distance to the N-terminus (Figure 3F) would affect degradation. In other words, is there a minimal number of AA residues within AA2-9 that are needed for REV-ERBα to maintain WT-like stability?

Interestingly, relative to the WT (Figure 3G, lanes 1-6), faster degradation was readily detected even when only two amino acids were deleted (delAA2-3, lanes 7-12) from the N-terminus. Extending the deletion to six amino acids resulted in a similar faster degradation (delAA2-7, lanes 13-18), but none comparable to the highly unstable delAA2-9 (lanes 19-24), which could only be seen after a longer exposure. This drastic drop in stability of the protein suggested a minimum of two amino acids (N8N9)

are enough to delay protein degradation, but not to the extent when AA2-9 is present. These data suggested that AA2-9 blocks REV-ERBα from fast degradation by maintaining a proper distance between the N-terminus and sequence C-terminus to AA10 and onward. The presence of a minimal two out of the eight amino acids found in AA2-9 offers a weakened but discernable level of protection against degradation.

AA2-9 must be at the very N-terminus to exert its protective effect against degradation.

If the presence of AA2-9 from the N-terminus is the reason why REV-ERBα degradation is maintained at the WT level, mechanistically, it is possible that when it reaches the time of the day where REV-ERBα is no longer desired in the cells, a change in the WT conformation may occur in a specific way such that even though AA2-9 is physically there, it is no longer able to carry out the protective function, and degradation of the protein is accelerated. We explored this possibility and found that comparing to the WT (Figure 4B, lanes 1-6), the time course of degradation of a re-arranged REV-ERBα mutant (Figure 4A, mutant AA2-9insAA25; Figure 4B, lanes 19-24), was not different from that of delAA2-9 (lanes 7-12). Consistent with Figure 2, reversal of AA2-9 to AA9-2 at its original N-terminal location (Rev-AA9-2, lanes 13-18) was still WT-like. These results clearly showed that for AA2-9insAA25, although AA2-9 is near its native location, it is no longer protecting the protein from degrading like the WT, and thus behaving as if AA2-9 is not there (delAA2-9). These data suggested that AA2-9 must be resided at the very N-terminus in order for REV-ERBα to maintain WT-like stability, and a conformational change within the N-terminus may in some ways incapacitate AA2-9's degradation-impeding function. These results also lends support to the hypothesis that possible interactions within the first 25 amino acids of REV-ERBα could indeed function as a switch to alter the speed of degradation.

AA4-9 is the site of interaction with the E3 ubiquitin-ligase SPSB4

Knocking out REV-ERBα have two major important effects on mice. First, these mice exhibit significantly shorter circadian period length to WT mice when kept at constant darkness. Second, mouse to mouse variation in the period length is much higher in the knockout mice when compared to the WT (4). These results suggested the loss of REV-ERBα led to a propensity to have an inaccurate clock. Furthermore, we have demonstrated that when the level of the ubiquitin ligase SPSB4 was knocked down in U2OS cells, an increase in period length was observed, along with an apparent stabilization of REV-ERBα (13). These published results imply that the site of interaction with SPSB4 on REV-ERBα could potentially control or regulate the circadian period. To map the region on REV-ERBα that is required for its binding to SPSB4, we introduced MYC- or HA-epitope into the C-termini of SPSB4 and REV-ERBα. This is essential since there is no reliable anti-SPSB4 antibody, and some of the deletions introduced into REV-ERBα would inevitably remove the epitope that is the site of recognition by the commercially available anti-REV-ERBα antibody. A series of large truncation mutants that covers the entire 615 AAs of the protein were first prepared in REV-ERBα-MYC. SPSB4-HA was paired with various deletion mutants of REV-ERBα-MYC, in co-transfection experiments, followed by IP and western blots with anti-HA, anti-MYC, or anti-REV-ERBα antibody, where appropriate. As summarized in Figure 5, positive interactions between the two proteins are indicated by the "+" signs after the corresponding mutants. The first set of REV-ERBα-MYC deletion mutants (Figure 5A) helped narrow down the SPSB4-binding domain to the first 200 amino acids. The next set of REV-ERBα-HA mutants with smaller deletions were made and tested for binding to SPSB4-MYC, and the results narrowed down the binding to the first 50 amino acids (Figure 5B), as its removal from the two deletion mutants (REV-ERB51-400HA and REV-ERB100-400HA) abolished binding to SPSB4.

Next, we had more N-terminal deletion mutants to further localize the binding site for SPSB4. As shown in Figure 6A, these are full length REV-ERBα protein with only the indicated length of peptide deleted

(dashed-lines in the sequence). IP with anti-REV-ERBα antibody was successful in pulling down the WT and the indicated N-terminal mutants (lanes 5-8, around 75kD, marked by open arrowhead). Most importantly, although similar levels of SPSB4 were expressed (lanes 9-12, detected by anti-MYC antibody, around 25kD, marked by solid arrowhead), it was only brought down by the WT (lane 13) or the delAA10-25 mutant (lane 15) (also marked by the "+" sign yo yhe right of the corresponding sequence). These data suggest that SPSB4 was bound to AA2-9 (blue sequence), as its absence in delAA2-17 and delAA2-25 abolished the binding (lanes 14 and 16, also indicated by the "-" sign to the right of the sequence).

We then made use of the full-length REV-ERBα mutants with only two amino acids substitution (used in earlier experiment presented in Figure 2) to determine the sequence required for SPSB4 binding. As shown in Figure 6B, WT REV-ERBα and all the mutants were brought down by IP with anti-REV-ERBα antibody (lanes 19-24, marked by open arrowhead). Despite the detection of SPSB4-MYC in all the input samples (lanes 1-6, marked by solid arrowhead) and, consistent with the results in Figure 6A, binding to the WT protein was clearly detected (lane 7), but was abolished with delAA2-9 (lane 8). Out of the four substitution mutants (lanes 9-12), only T2T3AA was still able to bind with SPSB4 (lane 9, and indicated by the "+" sign to the right of the sequence). Importantly, T2T3AA was still highly susceptible to degradation induced by SPSB4 (Figure 6C, compare lanes 7-12 with lanes 1-6). Consistent with the loss of binding to SPSB4 (Figure 6B), N8N9AA became more resistant to degradation by SPSB4 (Figure 6C, compare lanes 19-24 with lanes 13-18). The combined data showed that SPSB4 binding site is located to a 6 amino acid peptide at AA-4-9.

Does AA2-9 affect ubiquitination of REV-ERBα stability?

Data from the previous sections (Figures 5 and 6) clearly demonstrated that AA4-9 is the binding site for the ubiquitin ligase SPSB4, but the removal of AA2-9 resulted in faster degradation (Figure 2), which is opposite to what expected when an ubiquitin ligase bindind site is removed. Furthermore, the efficient ubiquitination of K20R (Figure 1D) implicates possible N-terminal ubiquitination, it is therefore important to test if and how ubiquitination is affected when AA2-9 is deleted. Both WT and delAA2-9 (the sequences and their abilities to bind SPSB4 are shown in the bottom) were transfected into HEK293 cells, with (Figure 8, "+" lanes) or without ("-" lanes) co-transfection of a plasmid that expresses HA-tagged ubiquitin cDNA (HA-Ub). Cells were lysed and followed by immunoprecipitation (IP) with anti-REV-ERBα antibody (lanes 7-18). Western blot using anti-REV-ERBα antibody showed that both WT (lanes 7,8) and delAA2-9 (lanes 10,11) were successfully brought down by IP. Consistent with delAA2-9 being less stable, higher levels of WT were detected both in the input (compare lanes 1 and 2 to lanes 4 and 5), and the IP samples (compare lanes 7 and 8 to lanes 10 and 11). Meanwhile, endogenous REV-ERBα was undetectable in HEK293 cells transfected with the empty vector Sport6 ("S6" lanes 3, 6, 9, and 12). When anti-HA antibody was used in the western blot (lanes 13-18), bands appeared as ladders (marked by bracket) were detected only in those lanes where HA-Ub were also co-transfected (lanes 16 and 18). These bands all have higher molecular weight than that of REV-ERBα (around 75kD, bands at 50kD are immunoglobulin heavy chain), suggesting that they are REV-ERBα with increasing numbers of ubiquitin molecules attached, as each additional ubiquitin molecule would increase the size of the protein by 8kD. The absence of these ladders in the HEK293 cells transfected with Sport6 (lanes 13 and 14) further confirmed their specificity. Therefore, although there was less delAA2-9 immunoprecipitated than the WT protein (compare lane 10 to lane 8), the ladder of bands detected in delAA2-9 (lane 18) were very similar to those detected with the WT (lane 16). It is difficult to make accurate quantitation from an immunoprecipitation experiment, but the results suggested a higher tendency for delAA2-9 to be ubiquitinated.

Discussions

We and others have investigated how various ubiquitin ligases contribute to the degradation of REV-ERBα, and their effects on the circadian clock (12-16). In this study, we focused on trying to understand the central events that need to happen to REV-ERBα protein itself for degradation to take place. As ubiquitin ligases are supposed to drive degradation by initiating the whole process through ubiquitination of the target protein on certain lysine residue(s), we were surprised by the results that lysines are not required for ubiquitination and degradation of REV-ERBα (Figure 1), as the ε-amino group on lysine is believed to be the common site where ubiquitin attaches. Literature search returned a few proteins that were reported to undergo lysine-independent degradation (21, 22). As suggested by some of these studies, the most likely site of attack by ubiquitin on their lysine-less mutant proteins, all of which are devoid of ε-amino groups, would be the free α-amino group locate at the N-terminus (23-26). The fact that K20R was readily ubiquitinated (Figure 1D) suggested that REV-ERBα may be added to this short list of a dozen or so proteins (27). However, one caveat of these reported N-terminal ubiquitinated proteins is that they could only be demonstrated by using an in vitro translation system, where the free α-amino group of the N-terminal methionine could be modified and blocked from potential ubiquitination in a cell-free ubiquitination assay. There is no easy way to modify the N-terminus of a freshly translated protein in vivo without affecting its expression, this is further complicated by possible effects mediated by the N-end rule of degradation (28), which recently was renamed as N-degron rule (29). These technical difficulties may be reasons why there are not many follow-up studies or other proteins reported to use such N-terminal ubiquitination mechanism. In recent years, there have been renewed interests in lysine-independent ubiquitination and their effects, many of which however, are not related to degradation (30).

The efficiently ubiquitinated K20R (Figure 1D) and several N-terminal ubiquitination studies (23-26) guided us to investigate the possible effects of small deletions at the N-terminus. It was intriguing to see the big change in stability between delAA2-9 and delAA2-17 (Figure 2), but these results provided a first glimpse into how this region may control the stability of REV-ERBα.

When AA2-9 was deleted, the protein became unstable (Figure 2), suggesting that it plays an important role in maintaining the protein in a relatively stable (WT) conformation, such that it can carry out its functions. The similarly unstable re-aligned mutant (AA2-9insAA25, Figure 4) indicated that AA2-9 must be located at its native position, at the very N-terminus, for its degradation-impeding function. The lack of specific sequence requirement for AA2-9 to help maintain the WT-like stability (Figure 3) may appear puzzling. However, others have described proteins that were targeted through a ubiquitin-independent proteasomal degradation pathway (31-33), mostly attributed to an intrinsic disordered region (34-37). Intrinsic disordered region has gained a lot of interest in recent years (37), as it is very flexible and has the potential to assume many different possible structures, through post-translational modification, or various intra- and inter-molecular interactions, with other regions on the same or different proteins. When the REV-ERBα protein sequence was subjected to a context-dependent prediction for protein disorder (38), indeed the first 100 AAs are predicted to be largely disordered (Figure 8, the higher the Score is above 0.5 on the Y-axis, the higher possibility of being disordered). This possibility may explain why small substitution and even altering the orders without changing the composition of AA residues within AA2-9 did not affect the protein stability (Figure 3A-E). On the other hand, smaller deletions, delAA2-3 and AA2-7 resulted in slightly faster degradation relative to the WT protein (Figure 3G and 3F), but not to the extent of delAA2-9, suggesting the degradation-protecting function is length dependent. AA2-9 is perhaps optimal for the protective effect, while shortened length still maintains a weaken but discernable activity. This in a certain way is consistent with the possible N-terminal ubiquitination, although we did not have direct evidence.

Interestingly, when the first 50 amino acids of the two REV-ERB(α and β) proteins are aligned (Figure 8A), in place of the AA2-9 of REV-ERBα, which is 8AAs in length, there are only 3AAs in the equivalent region of REV-ERBβ (AA2-4, blue sequence). The sequence that follows (AA10-25 on REV-ERBα) is well conserved on REV-ERBβ (AA 5-20, red and yellow). The data we have obtained in the current study could explain two observations on REV-ERBβ. First, as the blue sequence in REV-ERBα is protective against degradation and a shortened blue sequence is less capable in such protection (Figure 3F

and 3G), this may explain the inherent property of REV-ERBβ being a faster degrading protein than REV-ERBα. It is noteworthy that the small change in the blue sequence between REV-ERBα and REV-ERBβ translates into a readily detectable change from a high-likelihood of disordered region (38) in REV-ERBα to become low-liklihood in REV-ERBβ (Figure 8B, positions of the first 20 AAs are marked by the green vertical bar for the two proteins, matched to the sequences shown in Faigure 8A). Second, unlike REV-ERBα, REV-ERBβ was known to be resistant against degradation induced by SPSB4 (12), the mapping of SPSB4-binding to the blue sequence (Figure 5 and 6) explains such selective targeting activity of SPSB4 on REV-ERBα.

At first sight, the mapping of the SPSB4 binding site to AA4-9 is counterintuitive, in that removal of a E3-binding motif should result in a more stable protein. This contradicts the fact that deleting AA2-9 from the WT resulted in a faster degradation (Figure 2). It is unclear at this moment how to account for these apparently contradictory results, but these findings certainly indicate a more complicated mechanism of regulating REV-ERBα degradation. One possible explanation is that AA2-9 provides two separate functions. First, it serves as the binding site to recruit SPSB4, thus initiating the first step of ubiquitination to mark and prime the protein for its subsequent interaction with the 26S proteasome. Second, AA2-9 at the N-terminus may function to mask and impede (39) a peptide sequence that is a potential proteasome initiation region (31-33), which when exposed, will result in one or more of the following events, accelerated interaction with the proteasome, unfolding of the protein, and translocation into the pore of catalytic core of the proteasome (18,19), where the actual degradation takes place (40, 41). Weakened masking effects may also explain the weaker but discernable degradation-protective effects observed with the smaller deletions (delAA2-3, delAA2-7) as compared to delAA2-9 (Figure 3F and 3G). A potential site of such a proteasome initiation region on REV-ERBα may be AA10-17 or extending to AA10-25, which cloud explain why the delAA2-17 mutant became a very stable protein and even MG132 resistant (Figure 2), as both the SPSB4-binding capacity (AA2-9) and the proteasome initiation potential have been removed. The stability of the re-positioned mutant (AA2-9insAA25, Figure 4) being like delAA2-9 suggested that the realignment of this region may have disrupted how different elements within AA1-25 interact with each other, thus affecting the overall stability of REV-ERBα. The stability of many mutants in AA10-25 are now being studied to further understand its involvement in regulating the degradation process.

In light of our findings, it may be important to consider the degradation of REV-ERBα into two separate but inter-dependent processes, namely the regulation of the steady-state level of REV-ERBα and regulation of degradation driven by ubiquitin-ligases. It is possible that at the steady-state level of ubiquitin ligases in the cells, SPSB4 may not be able to recognize the binding site (AA4-9) due to the complicated interactions within the first 25AAs, or even when it is able to bind and promote ubiquitination, it is not able to proceed further along the subsequent steps of the degradation process, where the second function (degradation-impeding) of AA2-9 is now in control. Under this idea, other ubiquitin ligases may play a more essential role for the general maintenance of REV-ERBα, perhaps reflected by the stronger REV-ERBα-degrading activity of SIAH2 (Figure 1E). In addition, this may be the reason why delAA2-9 is still ubiquitinated with high efficiency (Figure 7) even when SPSB4-binding is eliminated. It is also possible that an increase in the level of SPSB4 at an appropriate time of the day may initiate a rapid elimination of REV-ERBα, thus controlling the time span of REV-ERBα in the cells.

The E3 ligase UBE2W, was the first E3 shown to promote N-terminal ubiquitination (42-44). A recent study identified 73 putative substrates of UBE2W (45), and most of which are predicted to have disordered N-termini. Among these were UCHL1 and UCHL5, two related deubiquitinases, that were identified as targets of N-terminal ubiquitination (45). Our mapping of the SPSB-4 binding site to the N-terminus of REV-ERBα (Figures 5 and 6), a region predicted to be intrinsically disordered (Figure 8), and the possible N-terminal ubiquitination (Figure 1), are features found on some substrates of UBE2W (42-45). These similarities in some ways validate the importance of the degradation control region in regulating REV-ERBα stability. Nevertheless, a major difference must be noted in that UBE2W only conjugates a single ubiquitin (mono-ubiquitination) onto its substrate (44, 45), and N-terminal

ubiquitination by UBE2W is not a strong signal for degradation, instead it seems to modulate the deubiquitinase function of those two substrates (45). In contrast, REV-ERBα was clearly poly-ubiquitinated (Figure 1) and degraded.

In conclusion, we have several interesting findings on the mechanisms of regulating REV-ERBα degradation. This includes lysine-independent ubiquitination and degradation, which implies perhaps N-terminal ubiquitination. The properties of these regulatory elements fit into a general theme of how degradation is controlled for many different proteins (46-48), but they appear to be all packaged into the first 25AAs at the N-terminus for REV-ERBα. The degradation blocking activity of AA2-9 appears to be non-sequence specific but length dependent, explainable by the composition of these amino acids that are predicted to be an intrinsic disordered region. Another function is its ability to bind the ubiquitin ligase SPSB4. These two apparently contradictory functions likely depend on how sub-segments within these first 25AAs interact with each other. Recently, Cryo-EM was able to resolve the detailed interactions (49-51) of various components with the proteasome throughout the degradation process. Similar approach would help the understanding of the structural changes that may be the results of various possible interactions among different segments within the N-terminal AA1-25, as well as SPSB4, and how these interactions actually control the degradation process.

The mapping of the SPSB4 binding site to AA4-9 of REV-ERBα is exciting (Figures 5 and 6), since our previous experiments showed that SPSB4-knockdown will result in the stabilization of REV-ERBα, as well as a longer circadian period (13). The shortfall of these ubiquitin ligase knockdown experiments is that one can always argue that the observed effects may be due to other possible targets of the ubiquitin ligase. Now, we can directly mutate the specific binding site on REV-ERBα and observe its effect on the circadian period, and in the future, even in animal's behavior and metabolism. Overall, it is important and very exciting to find this degradation-control domain, as it opens up the possibility to study how REV-ERBα existence in the cells is only limited to a specific time interval in the day (ZT6 to ZT10).

Acknowledgement
This work is supported by NIH NIGMS grants GM109861 and GM127044 to Jason P. DeBruyne, RCMI grant U54MD007602 to Ting-Chung Suen, as well as in part by NIH NINDS grant U54 NS083932 and NIH NIMHD grants 8G12MD007602, 8U54MD00758, 1G20RR031196, S21MD000101, C06RR18386 to Morehouse School of Medicine.

Disclaimer
The content is solely the responsibility of the authors and does not necessarily represent the official view of the National Institute of Health.

Conflict of Interest
The authors declare that they have no conflicts of interest with the contents of this article.

Reference

1. Takahashi, J.S. and Lowrey, P.L. (2000) Genetics of the mammalian circadian system: photic entrainment, circadian pacemakers mechanisms, and posttranslational regulation. *Annu. Rev. Genet.* **34**, 533-55
2. Mohawk, J.A., Green, C.B., and Takahashi, J.S. (2012) Central and peripheral circadian clocks in mammals. Annu. Rev. *Neuroscience* **35**, 445-462
3. Partch, C.L., Green, C.B., Takahashi, J.S. (2014) Molecular architecture of the mammalian circadian clock. Trends in *Cell Biol*. **24(2)**, 90-99
4. Preitner, N., Damiola, F., Lopez-Molina, L., Zakany, J., Duboule, D., Albrecht, and Schibler, U. (2002) The orphan nuclear receptor REV-ERBα controls circadian transcription within the positive limb of the mammalian circadian oscillator. *Cell* **110**, 251-260
5. Bugge, A., Feng, D., Everett, L.J., Briggs, E.R., Mullican, S.E., Wang, F., Jager, J., and Lazar, M.A. (2012) Rev-erbα and Rev-erbβ coordinately protect the circadian clock and normal metabolic function. *Genes & Dev* **26**, 657-667
6. Cho, H., Zhao, X., Hatori, M., Yu, R.T., Barish, G.D., Lam, M.T., Chong, L.-W., DiTacchio, L., Atkins, A.R., Glass, C.K., Liddle, C., Auwerx, J., Downes, M., Panda, S. (2012) Regulation of circadian behaviour and metabolism by REV-ERB-α and REV-ERB-β. *Nature* **485**, 123-127.
7. Kormann B., Schaad, O., Bujard, H., Takahashi, J.S., and Schibler, U. (2007) System-driven and oscillator-dependent circadian transcription in mice with a conditionally active liver clock. PLOS Biol. **5(2),** e34.
8. Kerscher O., Felberbaum, R., and Hochstrasser M. (2006) Modification of proteins by ubiquitin and ubiquitin-like proteins. Annu. Rev. Cell Dev. Biol. **22,** 159-180
9. Schwartz A.L. and Ciechanover, A. (2009) Targeting ptoteins for destruction by the ubiquitin system: implications for human pathobiology. *Annu. Rev. Pharmocol. Toxicol.* **49**, 73-96
10. Varshavsky, A. (2012) The ubiquitin system, an immense realm. *Annu. Rev. Biochem.* **81**, 167-176
11. Zheng N. and Shabek, N. (2017) Ubiquitin ligases: structure, function, and regulation. Annu. Rev Biochem. **86,** 129-157.
12. DeBruyne, J.P., Baggs, J.E., Sato, T.K., and Hogenesch, J.B. (2015) Ubiquitin ligase Siah2 regulates RevErbα degradation and the mammalian circadian clock. Proc. Natl. Acad. Sci. USA **112,** 12420-12425.
13. Mekbib, T., Suen, T.-C., Rollins-Hairston, A., and DeBruyne, J.P. (2019) The E3 ligases Spsb1 and Spsb4 regulate RevErba degradation and circadian period. J. Biol. Rhythms **34,** 610-621.
14. Mekbib T, Suen TC, Rollins-Hairston A, Smith K, Armstrong A, Gray C, Owino S, Baba K, Baggs JE, Ehlen JC, Tosini G, DeBruyne JP. (2022) The ubiquitin ligase SIAH2 is a female-specific regulator of circadian rhythms and metabolism. PLoS Genet. 2022 Jul 5;18(7):e1010305. doi:10.1371/journal.pgen.1010305. eCollection 2022 Jul.
15. Yin, L., Joshi, S., Wu, N., and Lazar, M.A. (2010) E3 ligases Arf-bp1 and Pam mediate lithium stimulated degradation of the circadian heme receptor Rev-erbα. Proc. Natl. Acad. Sci. USA **107,** 11614-11619.
16. Zhao, X., Hirota, T., Han, X., Cho, H., Chong, L.-W., Lamia, K., Liu, S., Atkins, A.R., Banayo, E., Liddle, C., Yu, R.T., Yates III, J.R., Kay, S.A., and Downes, M. (2016) Circadian amplitude regulation via FBXW7-targeted REV-ERBα degradation. Cell **165,** 1-14.
17. Finley, D. (2009) Recognition and processing of ubiquitin-protein conjugates by the proteasome. *Annu. Rev Biochem.* **78,** 477-513
18. Collins, G.A. and Goldberg, A. (2017) The logic of the 26S proteasome. Cell **169,** 792-806.
19. Bard, J.A.M., Bashore, C., Dong, K.C., and Martin, A. (2019) The 26S proteasome utilizes a kinetic gateway to prioritize substrate degradation. Cell **177,** 286-298.

20. Kim, W., Bennett, E.J., Huttlin, E.L., Guo, A., Li, J., Possemato, A., Sowa, M.E., Rad, R., Rush, J., Comb, M.J., Harper, J.W., and Gygi, S.P. (2011) Systematic and quantitative assessment of the ubiquitin-modified proteome. Mol. Cell **44,** 325-340.
21. Erales, J. and Coffino, P. (2014) Ubiquitin-independent proteasomal degradation. Biochimica et Biophysica Acta 1843, 216-221.
22. Ben-Nissan, G. and Sharon M. (2014) Regulating the 20S proteasome ubiquitin-independent degradation pathway. Biomolecules **4,** 862-884.
23. Reinstein, E., Scheffner, M., Oren, M., Ciechanover A., and Schwartz, A. (2000) Degradation of the E7 human papillomavirus oncoprotein by the ubiquitin-proteasome system: targeting via ubiquitination of the N-terminal residue. Oncogene **19,** 5944-5950.
24. Ikeda, M., Ikeda, A., and Longnecker (2002) Lysine-independent ubiquitination of Epstein-Barr virus LMP2A. Virol. **300,** 153-159.
25. Breitschopf, K., Bengal, E., Ziv, T., Admon, A., and Ciechanover A. (1998) A novel site for ubiquitination: the N-terminal residue, and not internal lysines of MyoD, is essential for conjugation and degradation of the protein. The EMBO J. **17 (20),** 5967-5973.
26. Fajerman, I, Schwartz, A.L., and Ciechanover A. (2004) Degradation of the Id2 developmental regulator: targeting via N-terminal ubiquitination. Biochemical and Biophysical Res. Communications **314,** 505-512.
27. Ciechanover A. and Ben-Saadon, R. (2004) N-terminal ubiquitination: more protein substrates join in. Trends in Cell Biol. **14(3),** 103-106.
28. Tasaki, T. Sriram, S.M., Park, K.S., and Kwon, Y.T. (2012) The N-end rule pathway. Annu. Rev. Biochem. **81,** 261-289.
29. Varshavsky A. (2019) N-degron and C-degron pathways of protein degradation. Proc. Natl. Acad. Sci. **116,** 358-366.
30. McClellan, A.J., Laugesen, S.H., and Ellgaard, L. (2019) Cellular functions and mechanisms of non-lysine ubiquitination . Open Biol. 190147. http://dx.doi.org/10.1098/rsob.190147
31. Fishbain, S., Prakash, S., Herrig, A., Elasser, S., and Matouschek, A. (2011) Rad23 escapes degradation because it lacks a proteasome initiation region. Nature Communications **2,** 192.
32. Alvarez-Castelao, B., Losada, F., Ahicart, P. and Castano, J.G. (2013) The N-terminal region of Nurr1 (a.a 1-31) is essential for its efficient degradation by the ubiquitin proteasome pathway. PLOS One **8(2),** e55999.
33. Yu, H., Gautam, A.K.S., Wilmington, S.R., Wylie, D., Martinez-Fonts., K., Kago, G., Warburton, M., Chavali, S., Inobe, T., Finkelstein, I.J., Babu, M.M. and Matouschek, A. (2016) Conserved sequence preferences contribute to substrate recognition by the proteasome. The J. Biol. Chem. **291(28)**, 14526-14539.
34. Pena, M.M.O., Melo, S., Xing, Y.-Y., White, K., Barbour, K.W., and Berger, F.G. (2009) The intrinsically disordered N-terminal domain of thymidylate synthase targets the enzyme to the ubiquitin-independent proteasome degradation pathway. The J. Biol. Chem. **284(46)**, 31597-31607.
35. Melo, S., Barbour, K.W., and Berger, F.G. (2011) Cooperation between an intrinsically disordered region and a helical segment is required for ubiquitin-independent degradation by the proteasome. The J. Biol. Chem. **286(42),** 36559-36567.
36. Tomita, T., Huibregtse, J.M., and Matouschek, A. (2020) A masked initiation region in retinoblastoma protein regulates its proteasomal degradation Nature Communications 11, 1-8.
37. Uversky, V.N. (2021) Recent developments in the fields of intrinsically disordered proteins: intrinsic disordered-based emergence in cellular biology in light of the physiological and pathological liquid-liquid phase transitions.

38. Erdős, G., Pajkos, M, and Dosztányi, Z. (2021) IUPred3: prediction of protein disorder enhanced with unambiguous experimental annotation and visualization of evolutionary conservation. Nucl. Acid Res. 49(W1), W297-W303.
39. Tomita, T., Huibregtse, J.M., and Matouschek (2019) A masked initiation region in retinoblastoma protein regulates its proteasomal degradation. Nature Communications 11, 1-8
40. Tomita, T. and Matouschek (2019) Substrate selection by the proteasome through initiation regions. Protein Science 28, 1222-1232.
41. Tomita, T. (2022) Structural and biochemical elements of efficiently degradable proteasome substrates. The J. Biochem. 171, 261-268 https://doi.org/10.1093/jb/mvab157
42. Scaglione, K.M., Venkatesha, B., Ashraf, N.S., Konen, J.R., Elenitoba-Johnson, K.S.J., Todi, S.V., and Paulson (2013) The ubiquitin-conjugating enzyme (E2) Ube2w ubiquitinates the N terminus of substrates. *J. Biol. Chem.* **288**, 18784–18788.
43. Tatham, M.H., Plechanovová, A., Jaffray, E.G., Salmen, H. & Hay, R.T. (2013) Ube2W conjugates ubiquitin to α-amino groups of protein N-termini. *Biochem. J.* **453**,137–145.
44. Vittal, V., Shi, L., Wenzel, D. *et al.* (2015) Intrinsic disorder drives N-terminal ubiquitination by Ube2w. *Nat Chem Biol* **11**, 83–89 https://doi.org/10.1038/nchembio.1700
45. Davies, C.W., Vidal, S.E., Phu, L., Sudhamsu, J., Hinkle, T.B., et al. (2021) Antibody toolkit reveals N-terminally ubiquitinated substrates of UBE2W. Nature Communications **12,** 4608. https://doi.org/10.1038/s41467-021-24669-6
46. Guharoy, M., Lazar, T., Macossay,-Castillo, and Tompa, P. (2022) Degron masking outlines degronons, co-degrading functional modules in the proteome. Communications Biol. 5, 445. https://doi.org/10.1038/s42003-022-03391-z
47. Sherpa, D., Chrustowicz, J., and Schulman, B.A. (2022) How the ends signal the end: Regulation by E3 ubiquitin ligases recognizing protein termini. Mol Cell, **82(8):**1424-1438. doi: 10.1016/j.molcel.2022.02.004. Epub 2022 Mar 4. PMID: 35247307; PMCID: PMC9098119.
48. Abdalla, O.H.M.H., Brittany, B., and Cheng, H.-Y. M. (2022) Death of a Protein: The Role of E3 Ubiquitin Ligases in Circadian Rhythms of Mice and Flies. Int. J. Mol. Sci. 2022, **23,** 10569. https://doi.org/10.3390/ijms231810569
49. de la Peña, A.H., Goodall, E.A., Gates, S.N., Lander, G.C., and Martin, A. (2018) Substrate-engaged 26S proteasome structures reveal mechanisms for ATP-hydrolysis driven translocation. Science. 2018 Nov 30;362(6418):eaav0725. doi: 10.1126/science.aav0725. Epub 2018 Oct 11.PMID: 30309908
50. Dong, Y., Zhang, S., Wu, Z., Li, X., Wang, W.L., Zhu, Y., Stoilova-McPhie, S., Lu, Y., Finley, D., and Mao, Y. (2019) Cryo-EM structures and dynamics of substrate-engaged human 26S proteasome. Nature. 2019 Jan;565(7737):49-55. doi: 10.1038/s41586-018-0736-4. Epub 2018 Nov 12.
51. Zhang S, Zou S, Yin D, Zhao L, Finley D, Wu Z, Mao Y. (2022) USP14-regulated allostery of the human proteasome by time-resolved cryo-EM. Nature 2022 May;605(7910):567-574. doi: 10.1038/s41586-022-04671-8. Epub 2022 Apr 27.

Figure Legends

Figure 1. Lysine-independent ubiquitination and degradation of REV-ERBα.
A. Wildtype (WT) mouse REV-ERBα is 615 amino acids (AAs) in length, where methionine (M) is at position 1. The 20 lysines (K) are distributed with respect to the DNA-binding (grey box, AA128-216) and ligand-binding (open box, AA419-612) domains, not drawn to scale. The 3 underlined Ks were shown to be ubiquitinated and published in an ubiquitinome study. All Ks are changed to Arginines (Rs) by *in vitro* mutagenesis and confirmed by sequencing in the K20R mutant. B. WT (lanes 1-8) or K20R (lanes 9-16) were transfected into HEK293 cells seeded in 24-well plate. 36-48 hours after transfection, cells were treated with cycloheximide for the indicated number of hours, and the Western blot was probed with anti-REV-ERBα antibody. The membrane was then probed with anti-glyceraldehyde-3-phosphate-dehydrogenase (GAPDH) antibody, and anti-βACTIN antibody, as loading controls. Lanes "M" were lysates from cells treated with MG132 for 6 hours (lanes 8 and 16). C. Intensity of REV-ERBα and GAPDH bands were measured with the Li-COR ImageStudio software. Quantities of the WT and R20 were normalized with GAPDH and all time points were expressed as a relative number to the respective time '0", which is set at 100. Results are the means of three experiments. D. WT or K20R were transfected into HEK293 cells with ("+" lanes) or without ("-" lanes) co-transfection of a plasmid that expresses a HA-tagged ubiquitin (HA-Ub). Lysates from transfected cells (lanes 1-6) were immunoprecipitated (IP) with an anti-REV-ERBα antibody (lanes 7-18). Western blots were probed with an anti-REV-ERBα (lanes 1-12) or anti-HA antibody (lanes 13-18). Bands that form a ladder are marked with a bracket on the right, representing REV-ERBα proteins that have increasing number of ubiquitin attached. E. K20R were co-transfected with Sport6 (lanes 1-8), Sport6-SPSB4 (lanes 9-16), or Sport6SIAH2 (lanes 17-24), into HEK293 cells. 36-48 hours after transfection, cells were treated with cycloheximide for the indicated number of hours, and the Western blot was probed with anti-REV-ERBα antibody. Lanes "M" were lysates from cells treated with MG132 for 4 hours (lanes 7, 15, and 23). Lanes "MC" were lysates from cells treated with both MG132 and cycloheximide for 4 hours (lanes 8, 16, and 24). Anti-GAPDH was used as a loading control.

Figure 2. Small deletions at the N-terminus alters REV-ERBα stability.
A. Wildtype (WT) REV-ERBα is drawn not to scale, with the first 25 amino acids (AAs) enlarged as three colored boxes, each 8AAs in length, after the methionine (M) at position 1, the rest of the protein is shown as a green ellipse. The sequence of the first 30AAs is shown underneath, color-matched to the 3 boxes, with dashed lines representing the deletions. B. WT (lanes 1-8) or the indicated mutants (lanes 9-24) were transfected into HEK293 cells seeded in 24-well plate. 36-48 hours after transfection, cells were treated with cycloheximide for the indicated number of hours, and the Western blot was probed with anti-REV-ERBα antibody. The membrane was then probed with anti-glyceraldehyde-3-phosphate-dehydrogenase (GAPDH) antibody, as a loading control. Lanes "M" were lysates from cells treated with MG132 for 10 hours (lanes 8, 16, and 24). C. Intensity of REV-ERBα and GAPDH bands were measured with ImageQuant LAS4000 software provided with the Luminescent Image Analyzer (FujiFim Medical System USA). Arbitrary units were used directly from the software.

Figure 3. AA2-9 at the N-terminus of REV-ERBα protects against fast degradation.
A. Only the first 30AAs of REV-ERBα is shown as in Figure 2, with the green sequence starting at AA26 representing the rest of the protein. AAs 2-3, 4-5, 6-7, or 8-9, were substituted with double alanine to generate the four mutants as shown. B. and C. WT (lanes 1-6) or the indicated mutants were transfected into HEK293 cells seeded in 24-well plate. 36-48 hours after transfection, cells were treated with cycloheximide for the indicated number of hours, and the Western blot was probed with anti-REV-ERBα antibody. The membrane was then probed with anti-glyceraldehyde-3-phosphate-dehydrogenase (GAPDH) antibody, as a loading control. The WT sample at time "0" (3B, lane 1) was also loaded into the gel in 3C as lane "0" for cross-membrane comparison. D. AA2-9 sequence was numbered on top as

such in the WT and re-arranged as shown in the two mutants. E. WT or mutants in 3D were transfected into HEK293 cells seeded in 24-well plate. 36-48 hours after transfection, cells were treated with cycloheximide for the indicated number of hours, and the Western blot was probed with anti-REV-ERBα antibody. The membrane was then probed with anti-glyceraldehyde-3-phosphate-dehydrogenase (GAPDH) antibody, as a loading control. F. Small deletions in AA2-9 were made as shown. G. WT or mutants in 3F were transfected into HEK293 cells seeded in 24-well plate. 36-48 hours after transfection, cells were treated with cycloheximide for the indicated number of hours, and the Western blot was probed with anti-REV-ERBα antibody. The membrane was then probed with anti-glyceraldehyde-3-phosphate-dehydrogenase (GAPDH) antibody, as a loading control. A long exposure was needed to detect delAA2-9 (lanes 19-24).

Figure 4. AA2-9 must be at the very N-terminus to protect REV-ERBα from fast degradation.
A. AA2-9 was introduced back into the deletion mutant dAA2-9, but was positioned to begin after the original AA25, as shown. B. WT (lanes 1-6) or the indicated mutants (lanes 7-24) were transfected into HEK293 cells seeded in 24-well plate. 36-48 hours after transfection, cells were treated with cycloheximide for the indicated number of hours, and the Western blot was probed with anti-REV-ERBα antibody. The membrane was then probed with anti-glyceraldehyde-3-phosphate-dehydrogenase (GAPDH) antibody, as a loading control. Lanes "M" were lysates from cells treated with MG132 for 3 hours (lanes 6, 12, 18, and 24).

Figure 5. Localization of SPSB4 binding to the N-terminus AA1-50 of REV-ERBα.
MYC- and HA-epitopes were inserted into the C-terminus of REV-ERBα and SPSB4, by in vitro mutagenesis. Various truncations and deletions were then introduced into REV-ERBα-MYC and REV-ERBα-HA to generate the deletion mutants as shown in 5A and 5B. A. WT REV-ERBα-MYC and large truncation mutants were co-transfected along with SPSB4-HA into HEK293. 36-48 hours after transfection, cell lysates were obtained and mixed with anti-MYC or anti-HA antibody, followed by immunoprecipitation (IP) with Protein A agarose beads. Western blots were probed with anti-REV-ERBα, anti-MYC antibody, or anti-HA antibody, where appropriate. Binding to SPSB4 are shown as "+" or "-" sign to the right of each construct. The combined data narrowed down the binding of SPSB4 to the first two hundred amino acids of REV-ERBα (AA1-200). B. WT REV-ERBα-HA and the indicated deletion mutants were co-transfected with SPSB4-MYC were co-transfection experiments into HEK293. 36-48 hours after transfection, cell lysates were obtained and mixed with anti-HA or anti-MYC antibody, followed by immunoprecipitation (IP) with Protein A agarose beads. Western blots were probed with anti-REV-ERBα, anti-MYC antibody, or anti-HA antibody, where appropriate. Binding to SPSB4 are indicated by "+" sign to the right each construct. The combined data narrowed the site of interaction to the first fifty amino acids of REV-ERBα (AA1-50).

Figure 6. AA4-9 at the N-terminus of REV-ERBα is the binding site for SPSB4.
A. WT Rev-ERBα and the indicated mutants (lanes 1-4) were transfected along with SPSB4-MYC, and cells lysates were obtained 36-48 hours after transfection. Immunoprecipitation was carried out (lanes 5-8) with an anti-REV-ERBα antibody. The western blots were probed with anti-REV-ERBα (lanes 1-8) or anti-MYC antibody (lanes 9-16). The positions of REV-ERBα and SPSB4 are marked with open and solid arrowhead, respectively. Binding and non-binding mutants are indicated by "+" and "-" signs, respectively, shown to the right of the sequence. The combined data narrowed down the binding of SPSB4 to AA2-9. B. Small double alanine substitution mutants of REV-ERBα, used previously in Figure 2, were tested in binding assay with SPSB4-MYC, as performed in 6A. Transfected cell lysates obtained and IP with anti-REV-ERBα antibody (lanes 7-12 and lanes 19-24). The western blots were probed with anti-MYC antibody (lanes 1-12) or anti-REV-ERBα antibody (lanes 13-24). The positions of REV-ERBα and SPSB4 are marked with open and solid arrowhead, respectively. C. The two mutants used in

experiment in 6B, T2T3AA (lanes 1-12) and N8N9AA (lanes 13-24) were transfected into HEK293 cells along with either Sport6 or SPSB4-MYC, as indicated. 36-48 hours after transfection, cells were treated with cycloheximide for the indicated number of hours, and the Western blot was probed with anti-REV-ERBα antibody. The membrane was then probed with anti-glyceraldehyde-3-phosphate-dehydrogenase (GAPDH) antibody, as a loading control. Lanes "M" were lysates from cells treated with MG132 for 3 hours (lanes 6, 12, 18, and 24). Expression of SPSB4 was detected by anti-MYC antibody, since the SPSB4 was tagged with a MYC-epitope at its C-terminus.

Figure 7. Deleting AA2-9, the binding site of SPSB4, did not have much effect on ubiquitination of REV-ERBα.
Sport6, WT, or delAA2-9 were transfected into HEK293 cells with ("+" lanes) or without ("-" lanes) co-transfection of a plasmid that expresses a HA-tagged ubiquitin (HA-Ub). Lysates from transfected cells (lanes 1-6) were immunoprecipitated (IP) with an anti-REV-ERBα antibody (lanes 7-18). Western blots were probed with an anti-REV-ERBα (lanes 1-12) or anti-HA antibody (lanes 13-18). Bands that form a ladder are marked with a bracket on the right, representing REV-ERBα proteins that have increasing number of ubiquitin attached. Sequences of WT and AA2-9 and their abilities to bind SPSB4 are shown in the bottom.

Figure 8. Difference in the N-termini between REV-ERBα and REV-ERBβ correlates with predicted intrinsic disordered region.
A. The first 50 amino acids of REV-ERBα between REV-ERBβ are shown, with the same color scheme that was used in this study. B. Profile of predicted disordered regions compared between REV-ERBα and REV-ERBβ, aligned with the respective full-length protein, shown in the bottom. The green bar in 8B matches those in 8A, which marks the position of the first 20 amino acids. All scores over 0.5 on the Y-axis predicts an intrinsic disordered region. Protein sequences of REV-ERBα and REV-ERBβ, were input into https://iupred3.elte.hu (38) to obtain the profiles.

Figure 1 Lysine-independent ubiquitination and degradation of REV-ERBα.

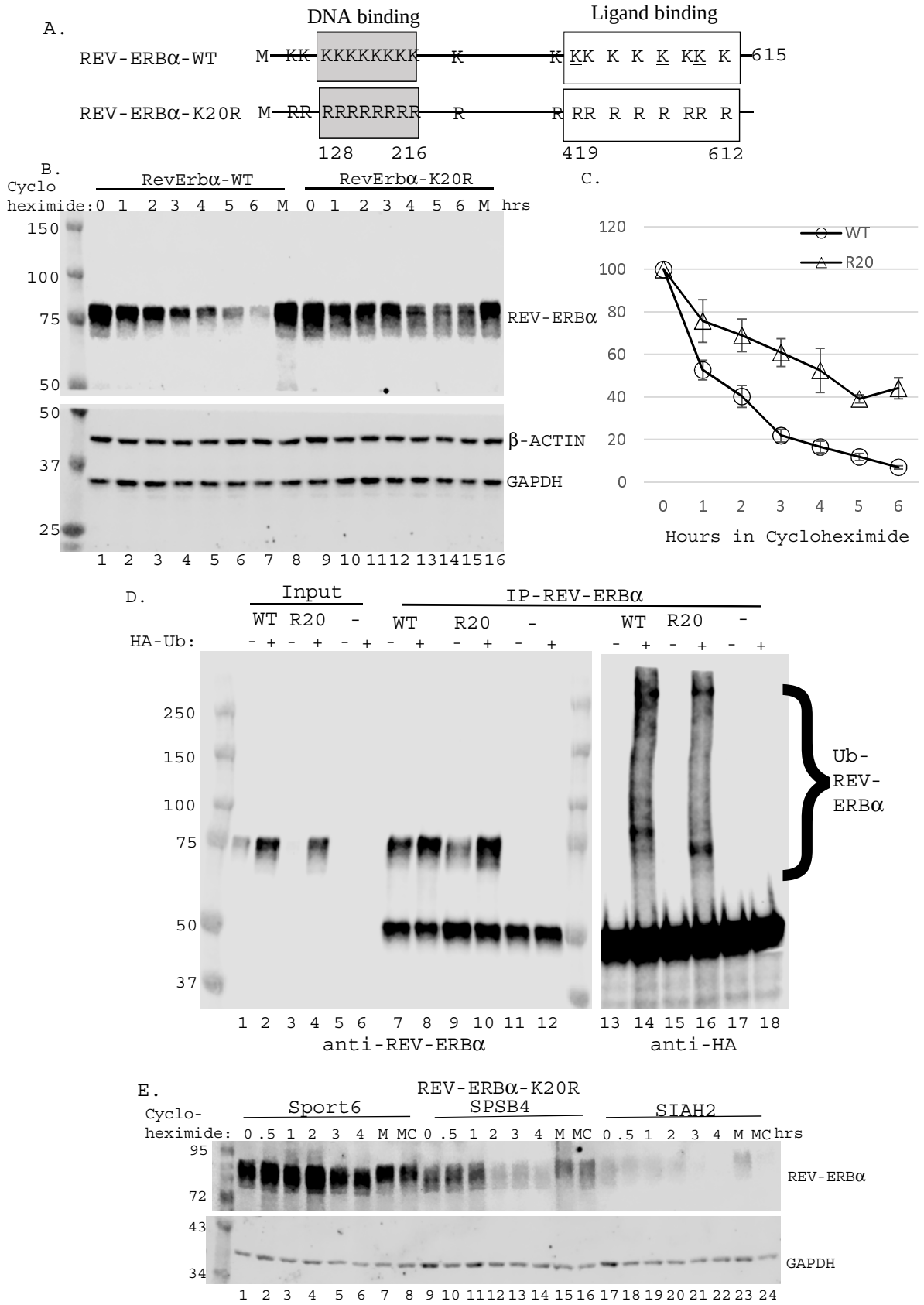

Figure 2. AA2-9 at the N-terminus of REV-ERBα protects against fast degradation.

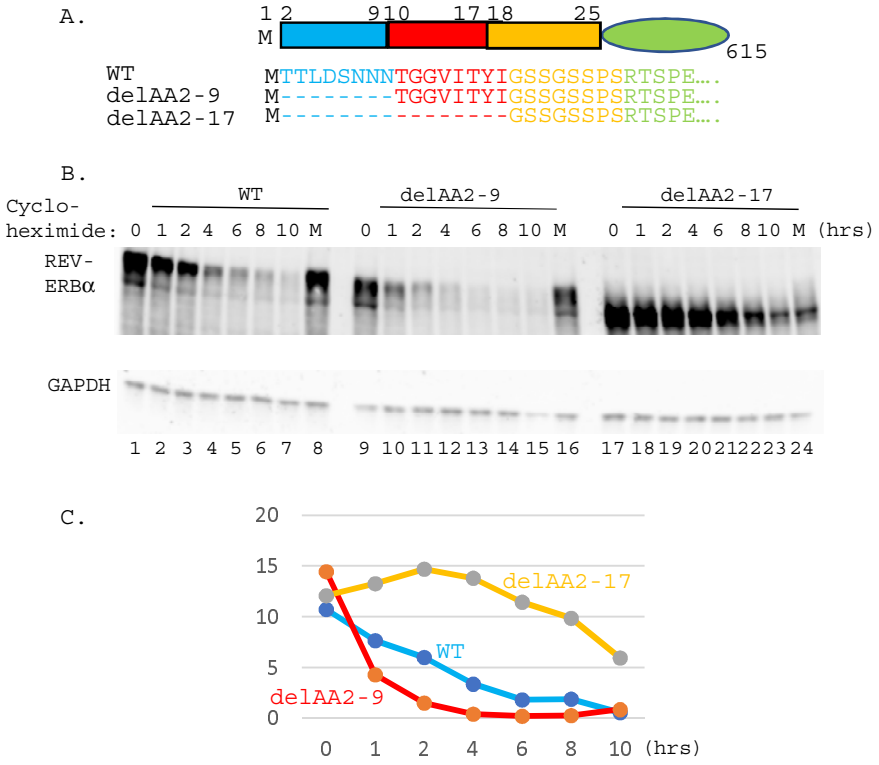

Figure 3. AA2-9 protects REV-ERBα against fast degradation.

A.

REV-ERBα

	1 2 3 4 5 6 7 8 9 10 ... 25
WT	MTTLDSNNNTGGVITYIGSSGSSPSRTSPE...
T2T3AA	MAALDSNNNTGGVITYIGSSGSSPSRTSPE...
L4D5AA	MTTAASNNNTGGVITYIGSSGSSPSRTSPE...
S6N7AA	MTTLDAANNTGGVITYIGSSGSSPSRTSPE...
N8N9AA	MTTLDSNAATGGVITYIGSSGSSPSRTSPE...

B.

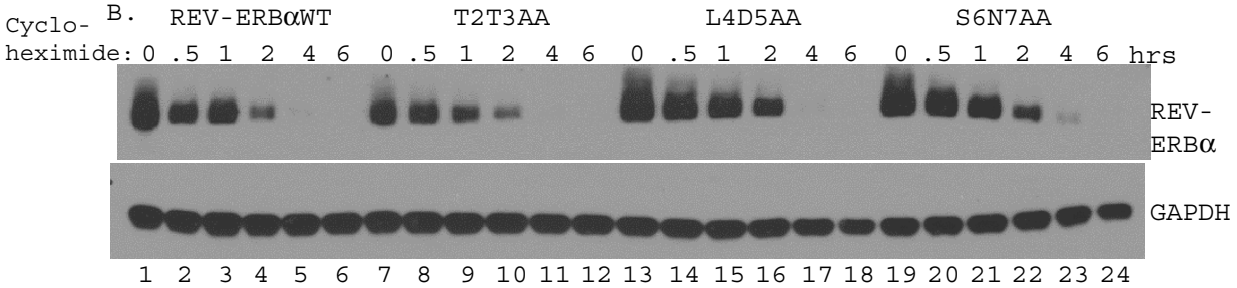

C.

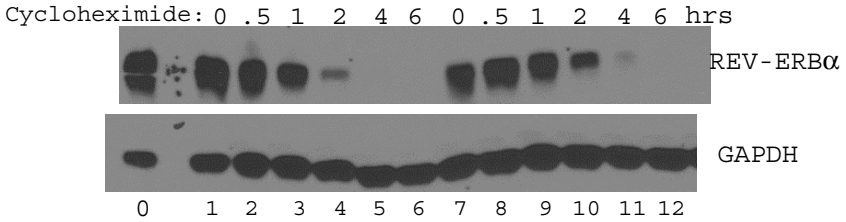

D.

	1 2 3 4 5 6 7 8 9 10 ... 25
WT	MTTLDSNNNTGGVITYIGSSGSSPSRTSPE...
RevAA9-2	1 9 8 7 6 5 4 3 2 10 MNNNSDLTTTGGVITYIGSSGSSPSRTSPE...
ScrambleAA2-9	1 9 2 8 3 7 4 6 5 10 MNTNTNLSDTGGVITYIGSSGSSPSRTSPE...

E.

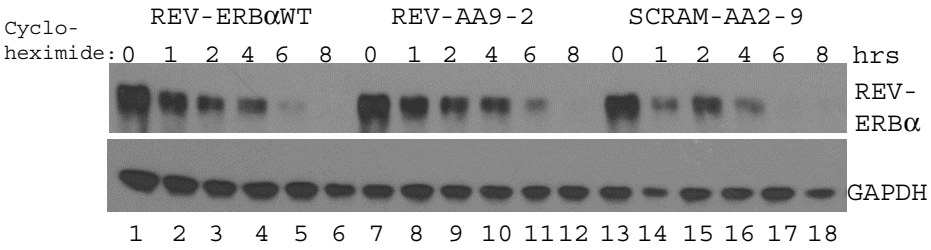

F.

	1 2 3 4 5 6 7 8 9 10 ... 25
WT	MTTLDSNNNTGGVITYIGSSGSSPSRTSPE...
delAA2-3	M--LDSNNNTGGVITYIGSSGSSPSRTSPE...
delAA2-7	M------NNTGGVITYIGSSGSSPSRTSPE...
delAA2-9	M--------TGGVITYIGSSGSSPSRTSPE...

G.

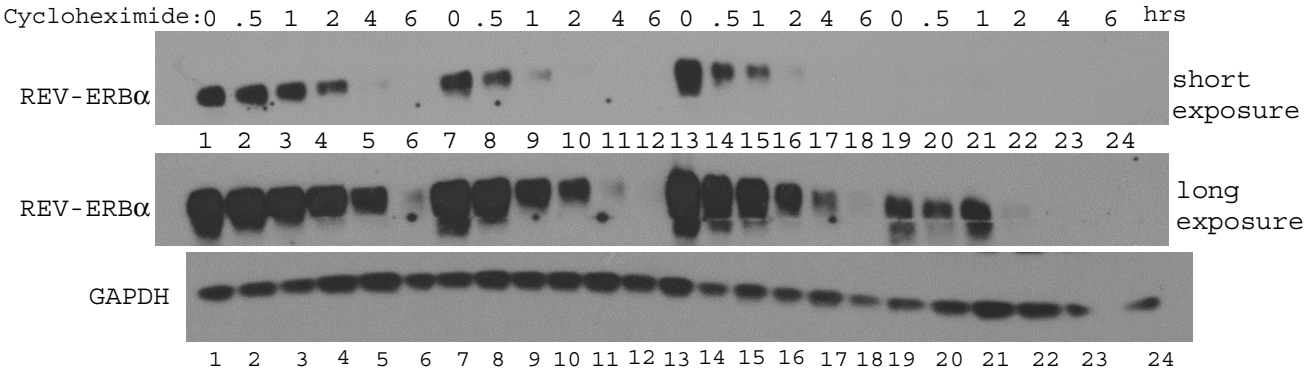

Figure 4. AA2-9 must be at the very N-terminus to protect REV-ERBα from fast degradation.

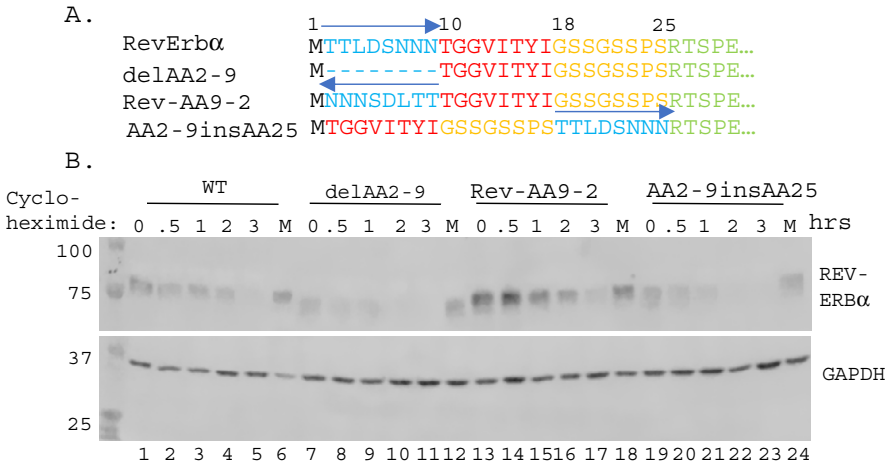

Figure 5 Localization of SPSB4 binding domain on RevErbα protein.

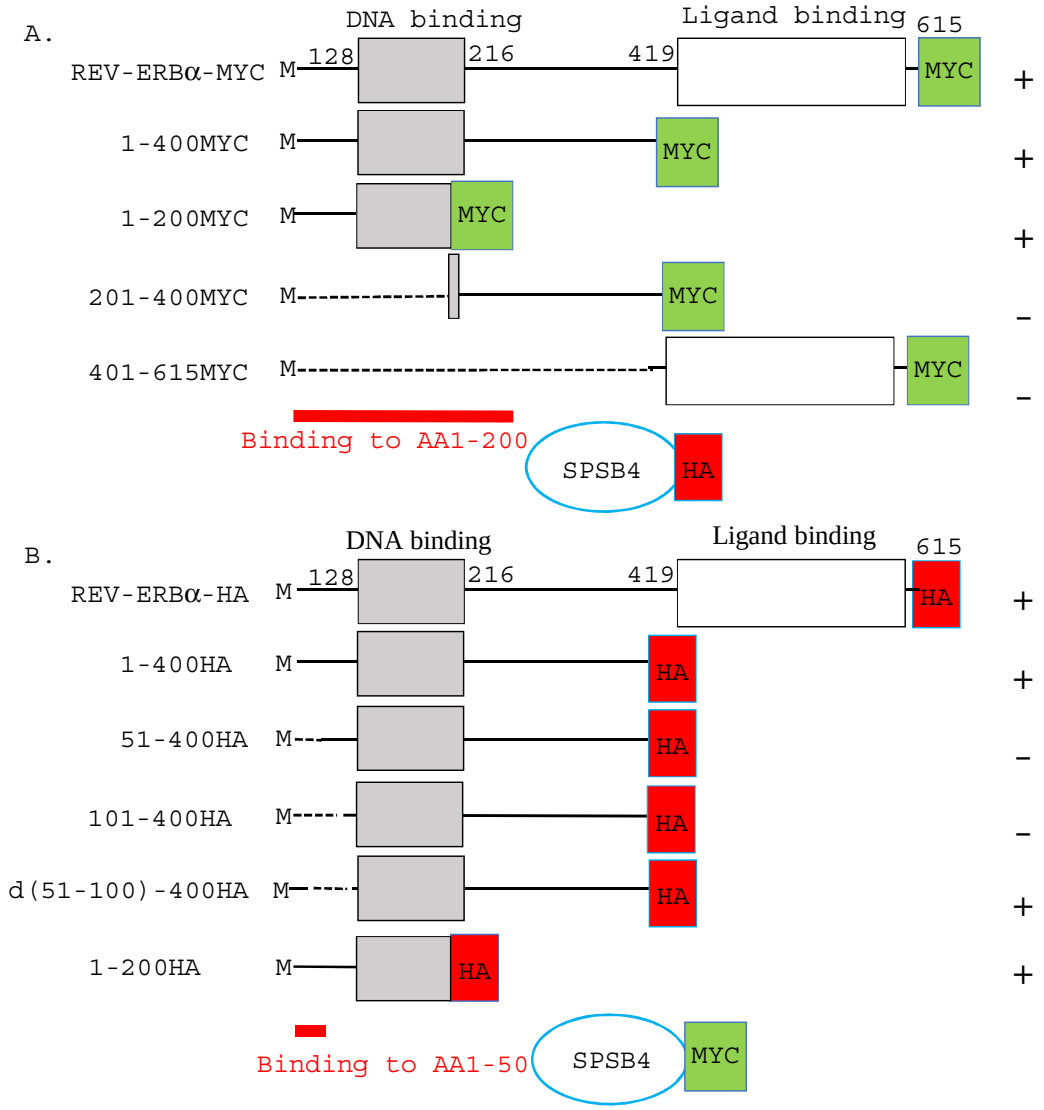

Figure 6 . Localization of SPSB4 binding to AA4-9 of REV-ERBα.

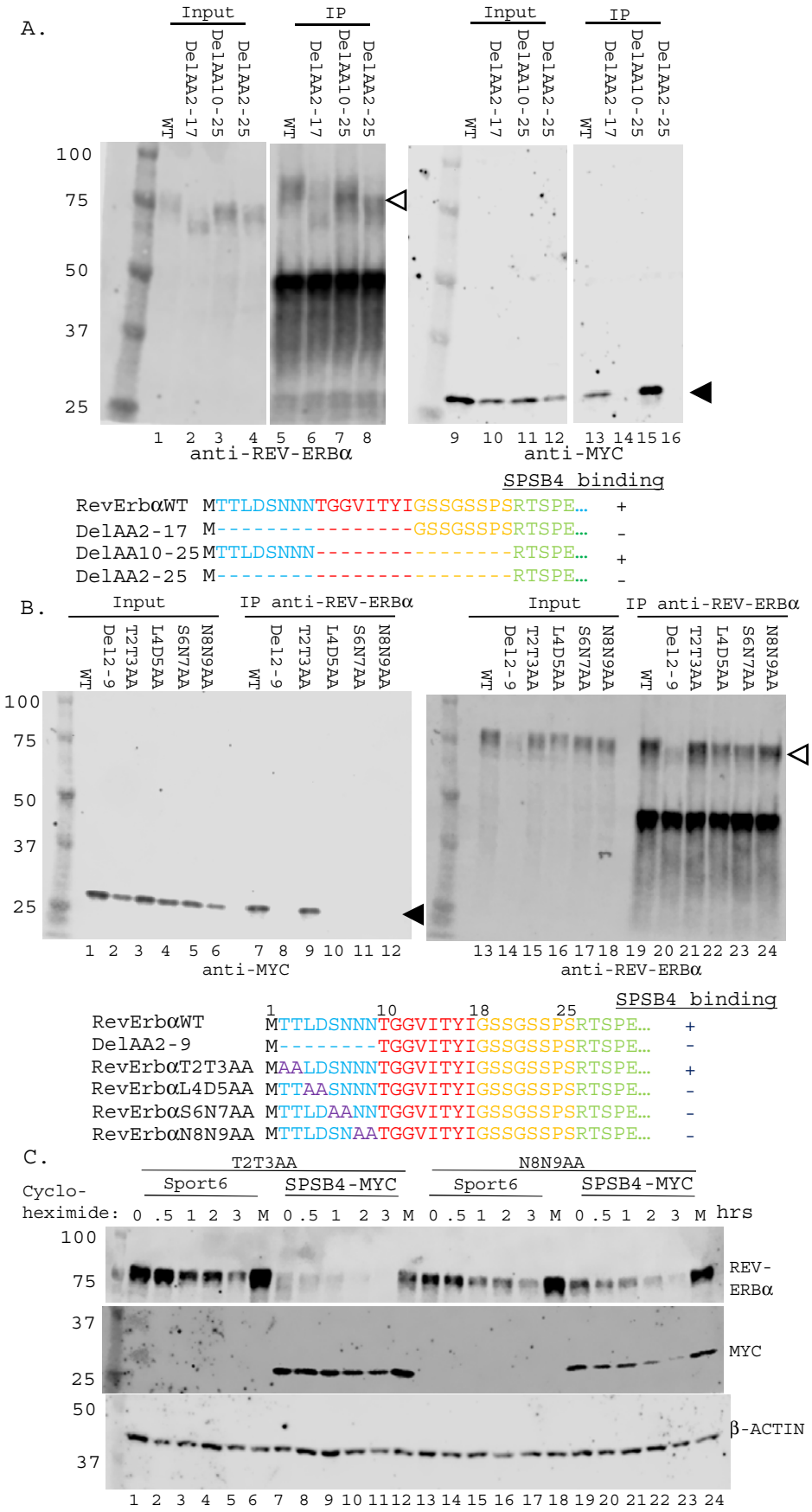

Figure 7. Deletion of SPSB4-binding site did not abolish ubiquitination of REV-ERBα.

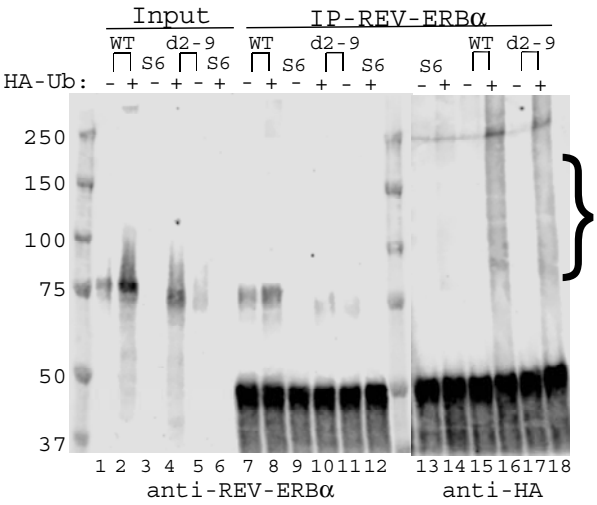

		SPSB4 binding
RevErbαWT	MTTLDSNNNTGGVITYIGSSGSSPSRTSPE…	+
DelAA2-9	M--------TGGVITYIGSSGSSPSRTSPE…	-

Figure 8. Difference in N-termini between REV-ERBα and REV-ERBβ correlates with predicted disordered region.

A.

RevErbα MTTLDSNNNTGGVITYIGSSGSSPSRTSPESLYSDSSNGSFQSLTQGCPTYFPPSPTGSL...

RevErbβ ME-L----NAGGVIAYISSSSSASSPASCHSEGSENSFQSSSSSVPSSPNSSNCDANGNPKN

B.
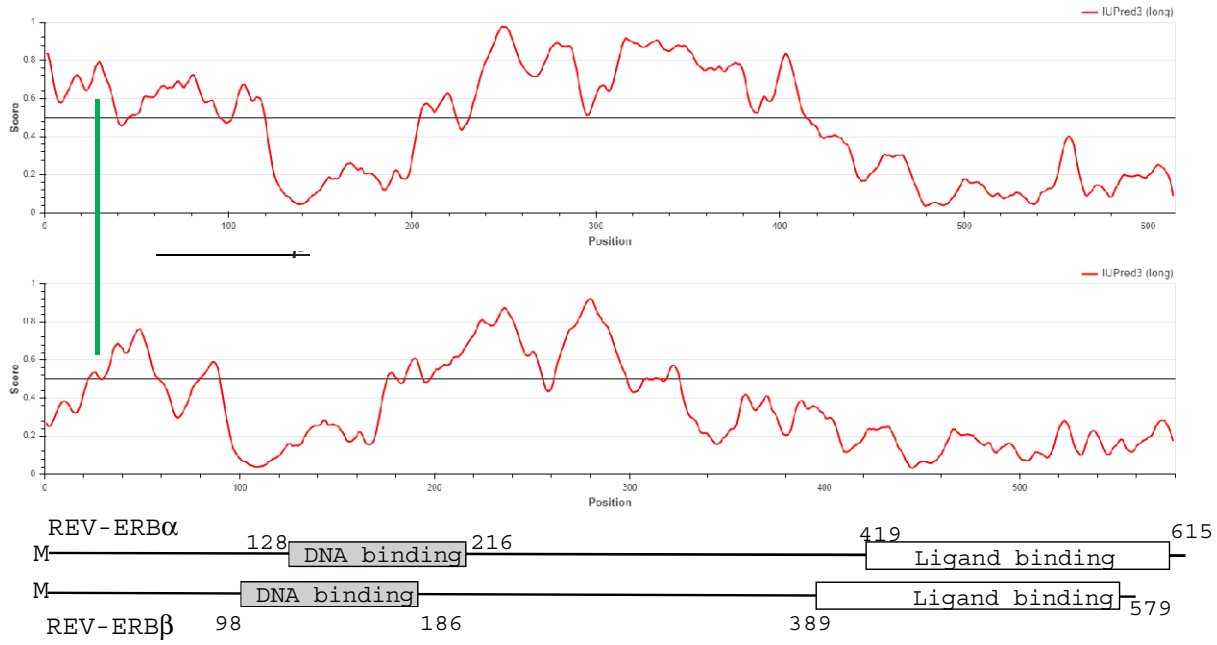
Human REV-ERBα